COMPACT TAG ANTENNA FOR METAL-MOUNTABLE APPLICATIONS IN THE UHF RFID PASSBANDS

CHOE SIU KIT

UNIVERSITI TUNKU ABDUL RAHMAN

COMPACT TAG ANTENNA FOR METAL-MOUNTABLE APPLICATIONS IN THE UHF RFID PASSBANDS

CHOE SIU KIT

A project report submitted in partial fulfilment of the requirements for the award of Bachelor of Electrical and Electronics Engineering with Honours

Lee Kong Chian Faculty of Engineering and Science
Universiti Tunku Abdul Rahman

May 2025

DECLARATION

I hereby declare that this project report is based on my original work except for citations and quotations which have been duly acknowledged. I also declare that it has not been previously and concurrently submitted for any other degree or award at UTAR or other institutions.

Name : Choe Siu Kit

ID No. : 2102311

Date : 27/4/2025

COPYRIGHT STATEMENT

This final year project report is submitted in partial fulfilment of the requirements for the degree of Bachelor of Electrical and Electrical Engineering with honours at Universiti Tunku Abdul Rahman (UTAR). This final year project report represents the work of the author, except where due acknowledgement has been made in the text. No part of this final year project report may be reproduced, stored, or transmitted in any form or by any means, whether electronic, mechanical, photocopying, recording, or otherwise, without the prior written permission of the author or UTAR, in accordance with UTAR's Intellectual Property Policy.

ACKNOWLEDGEMENTS

I would like to thank everyone who had contributed to the successful completion of this project. I would like to express my gratitude to my research supervisor, Prof. Lim Eng Hock for his invaluable advice, guidance and his enormous patience throughout the development of the research.

In addition, I would also like to express my gratitude to my seniors, Gene Ng Jinh Han and Tan Jiun Ian for their generous support and insightful suggestions which helped me overcome various challenges throughout my final year project.

ABSTRACT

This report presents the theoretical background, methodology, configuration of the proposed tag antenna, performance analysis and challenges encountered in developing the tag antenna. The aim is to design a compact and high-performance metal mountable tag antenna for omnidirectional radiation applications in the UHF RFID passbands. This project focuses on patch antenna structure that incorporates zeroth-order resonance (ZOR) principles to enhance performance while maintaining a compact form factor.

The study investigates the fundamental concepts of RFID systems and the impact of metal surfaces on antenna performance, as well as various approaches to overcome these challenges. Through a series of simulations using CST Studio Suite, design iterations were conducted to optimize the antenna's radiation pattern, gain, and impedance matching.

Overall, a compact UHF RFID tag antenna based on zeroth-order resonance (ZOR) is proposed for on-metal omnidirectional tag design. The proposed tag antenna consists of two identical patches, which are placed in the antipodal arrangement. Each patch is connected to the ground by a pair of elongated shorting stubs as well as a pair of open-ended side stubs. This structure can generate sufficient antenna impedance for achieving good conjugate matching, despite having a miniature size of 0.0824λ × 0.0824λ × 0.0098 λ (or 27 mm × 27 mm × 3.2 mm). A tag prototype has been fabricated, and achieves a constant read range of ~9.8 m (4 W EIRP) in all azimuthal directions with 4W EIRP when mounted on metal.

Keywords: UHF RFID tag; patch antenna; omnidirectional; on-metal; zeroth-order resonance

Subject Area: TK5101-6720 Telecommunication

TABLE OF CONTENTS

LIST OF TABLES

LIST OF FIGURES

LIST OF SYMBOLS / ABBREVIATIONS

c	velocity of the EM wave in vacuum, ms^{-1}
C_L	left-handed capacitance, F
C'_L	left-handed capacitance per unit length, Fm^{-1}
C_R	right-handed capacitance, F
C'_R	right-handed capacitance per unit length, Fm^{-1}
d	distance between the sides of resonator, m
$\vec{E}$	electric field, Vm^{-1}
f	frequency, Hz
G_r	gain of the reader antenna, unitless
G_t	gain of the tag antenna, unitless
$\vec{H}$	magnetic field, Am^{-1}
L_L	left-handed inductance, L
L'_L	left-handed inductance per unit length, m^{-1}
L_R	right-handed inductance, L
L'_R	right-handed inductance per unit length, Lm^{-1}
$\vec{M}_S$	magnetic currents, A
$\vec{n}$	unit normal vector, unitless
P_r	power received by the tag, W
P_t	power transmitted by the reader, W
R	resistance, Ω
r	radial distance from origin in spherical coordinate system, m
S_{11}	reflection coefficient, unitless
X	reactance, Ω
X_C	capacitive reactance, Ω
X_L	inductive reactance, Ω
x	position along horizontal axis in cartesian coordinate system, m
y	position along lateral axis in cartesian coordinate system, m
$\boldsymbol{Z}_A$	input impedance of the antenna, Ω
$\boldsymbol{Z}_c$	impedance of the chip, Ω
z	position along vertical axis in cartesian coordinate system, m

α	directional transmission beam angle, rad
β	phase constant, $radm^{-1}$
βl	electrical length, ^{o}
δ	loss angle, unitless
ε_r	relative permittivity, unitless
Φ	azimuthal angle in spherical coordinate system, ^{o}
λ	wavelength of the signal, m
ω	angular frequency, $rads^{-1}$
τ	power transmission coefficient, unitless
θ	polar angle in spherical coordinate system, ^{o}

UHF	ultra high frequency
RFID	radia frequency identification
ZOR	zeroth-order resonator
AMC	artificial magnetic conductor
CRLH-TL	composite right/left-handed transmission line
LH-TL	left-handed transmission line
RH-TL	right-handed transmission line
PCB	printed circuit board

CHAPTER 1

INTRODUCTION

1.1 General Introduction

In modern industrial and logistical systems, the demand for reliable and efficient identification technologies has led to the widespread adoption of RFID (Radio Frequency Identification) systems. UHF RFID (Ultra High Frequency RFID) are essential for facilitating wireless communication in asset tracking, inventory management, and automated data collection. These systems operate within the 902 to 928 MHz frequency range under FCC regulations, providing a balance between long read range and high data transfer rates (Finkenzeller, 2010).

Commonly, a dipole has been used for most tag antenna designs as they exhibit omnidirectional characteristics, which is useful for inventory management due to increased spatial coverage. However, mounting a dipole on a metallic object will experience degraded radiation efficiency (Nguyen et al., 2021) as well as a loss of its omnidirectionality. To address these challenges, various on-metal omnidirectional UHF tag antennas are proposed with a ground plane to omit the effects of the backing metal. Some designs include the use of a mushroom patch antenna (Tan et al., 2024) and a magnetic loop antenna (Lee et al., 2020). However, these designs have sizes that should be reduced further for better applicability in tagging purposes.

Recently, zeroth-order resonator (ZOR) antennas have emerged as a promising solution due to their miniaturization capability, and omnidirectional radiation characteristics (Li et al., 2020). By leveraging the unique properties of ZOR antennas, multiple ZOR based on-metal tag antenna designs have been proposed.

In this report, a ZOR antenna has been proposed for designing an on-metal tag antenna with omnidirectional characteristics. The proposed tag antenna consists of two identical patches, which are placed in the antipodal arrangement. It will be shown that this symmetrical design has an improved omnidirectionality. Also, multiple notches are introduced on the patch of the tag antenna to further reduce its physical size. This report presents the

theoretical background, methodology, configuration of the proposed tag antenna and performance analysis.

1.2 Importance of the Study

This study demonstrates the potential to achieve improved performance and compactness in UHF RFID tag antennas designed for use on metallic surfaces. In addition, the design process and findings may serve as a reference for future developments in compact antenna engineering, especially in the context of metal-mountable RFID systems. The techniques applied in this work can potentially be extended to other frequency bands or applications where antenna miniaturization and metal interference mitigation are required.

1.3 Problem Statement

In many practical applications, such as industrial asset tracking and warehouse inventory systems, RFID tag antennas are required to operate effectively when mounted on metallic surfaces while maintaining omnidirectional radiation characteristics. However, conventional antenna designs often experience significant performance degradation under these conditions. Firstly, typical tag antennas encounter a loss of omnidirectionality and a reduction in radiation efficiency when mounted on metal due to the interference caused by the reflective metal surface. Secondly, typical tag antennas provide insuffienct antenna impedance to achieve good conjugate matching when the size of antenna is small. This impedance mismatch further degrades the overall system performance by reducing power transfer efficiency.

1.4 Aim and Objectives

This project focuses on designing and developing a compact and high-performance metal-mountable zeroth-order resonator (ZOR) antenna for omnidirectional radiation applications. The antenna will operate within the UHF RFID frequency band (902 MHz to 928 MHz) and address the challenges associated with a loss of omnidirectionality and a reduction in radiation efficiency caused by metal surfaces as well as insufficient antenna impedance when the size of antenna is small. The objective of the project include:

- To propose a compact UHF RFID tag antenna with omnidirectional radiation characteristics, which is suitable for metal-mountable applications.
- To design an antenna capable of achieving a read range exceeding 5 meters in the whole azimuth plane.
- To reduce the dimension of the tag antenna as below 30mm × 30mm × 3.2mm.

1.5 Scope and Limitation of the Study

The focus of the study is to propose a new type of compact patch antenna design for UHF RFID tag. The result should improve the performance of the tag with a minimature size and cost, more flexibility and long read distance. However, there might be some limitations in this study, which may include:

- The study is lacked of detailed performance evaluation under various environmental condition.
- The study of this project is only focusing on a specific frequency range (902-928 MHz) only.
- The study of the project is focusing on low-cost condition. Thus, limited materials is allowed to use.

1.6 Contribution of the Study

Due to the reflective nature of metallic surfaces, metal-mounted RFID tag antennas typically exhibit directional radiation patterns. This limits their usability in applications that require full angular coverage. Therefore, if a compact tag antenna can maintain an omnidirectional radiation characteristics even when mounted on metal, it would greatly broaden the applicability of RFID technology.

This study presents a compact UHF RFID tag antenna based zeroth-order resonance (ZOR) principle. The proposed tag antenna is able to achieve omnidirectional radiation while mounted on metal. Furthermore, it has a small electrical size of 27 mm × 27 mm × 3.2 mm (0.0824 λ × 0.0824 λ × 0.0098 λ), and achieves a read range of approximately 9.8 meters. Compared to existing

omnidirectional tag antennas, the proposed design offers a more compact form factor and simplified structure without compromising performance.

1.7 Outline of the Report

The report is structured as follows: Chapter 2 presents a literature review and existing solutions. Chapter 3 outlines the methodology and project planning. Chapter 4 details the antenna configuration and evaluates the performance of the proposed tag antenna, including a parametric analysis of its impedance characteristics. Finally, Chapter 5 provides the conclusion and recommendations for future work.

CHAPTER 2

LITERATURE REVIEW

2.1 Introduction

This chapter provides a comprehensive review of the theoretical foundations and recent advancements relevant to the design of compact tag antennas, especially those for UHF RFID passbands. The review begins with an exploration of RFID technology and its critical components, followed by an in-depth analysis of antenna design principles, challenges, and solutions for metal-mountable applications. A detailed discussion of ZOR antennas is also included, highlighting their unique characteristics and potential in the context of RFID systems. Lastly, the chapter examines existing research on compact tag antennas, focusing on recent developments and areas requiring further exploration to inform the direction of the present study.

2.2 Overview of RFID Technology

Radio Frequency Identification (RFID) systems have transformed how industries manage assets and inventory by using electromagnetic fields to identify and track objects. The system typically consists of three main components: the RFID tag, the RFID reader, and the back-end system for data processing.

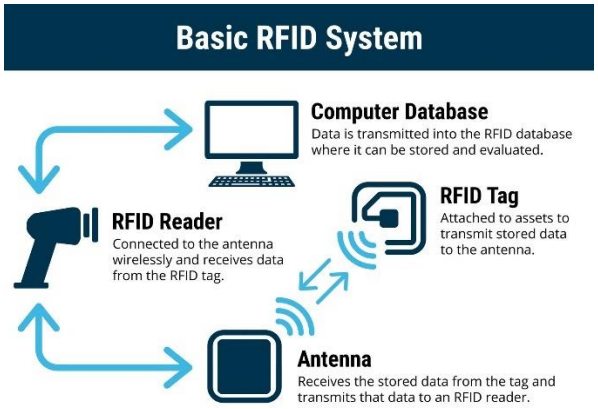

Figure 2.1: RFID System Overview. (TT Electronics, 2024)

RFID tags, also known as transponders, contain microchips for data storage and antennas for communication with RFID readers. Tags can be passive or active, depending on their power source. Passive tags, which are more common due to their low cost and long battery life, rely on the reader's energy for operation. Applications for passive RFID tags include retail inventory management and access control systems. (Chawla & Ha, 2007).

The RFID reader, or interrogator, sends a signal to the tag, which responds with its stored data. The reader processes this information and relays it to the back-end system, where the data is analyzed. RFID readers can be either fixed or mobile, with fixed readers being commonly used in warehouses or at entry/exit points, while mobile readers are used for on-the-go scanning in environments like retail stores and hospitals (Dobkin, 2012).

RFID systems operate across different frequency bands, such as Low Frequency (LF), High Frequency (HF), and Ultra High Frequency (UHF). Among these, UHF RFID has become increasingly popular due to its longer read range and faster data transfer rates (Want, 2006). Ultra High Frequency (UHF) RFID systems operate within the frequency range of 902 to 928 MHz under FCC regulations. This frequency band is part of the Industrial, Scientific, and Medical (ISM) spectrum, making it suitable for unlicensed use in various wireless communication applications, including RFID. UHF RFID is widely adopted due to its long read range, high data transfer rate, and ability to support multiple tag reads simultaneously, which is essential for large-scale applications like supply chain management, asset tracking, and inventory control (Finkenzeller, 2010).

UHF RFID systems typically utilize passive RFID tags, which rely on backscatter modulation to communicate with RFID readers. In this process, the reader transmits an electromagnetic wave that powers the passive tag and enables it to reflect and modulate the signal back to the reader. Unlike active RFID tags, passive tags do not require an onboard power source, making them more cost-effective and lightweight (Dobkin, 2012).

UHF RFID systems are highly sensitive to the surrounding environment, especially when placed near metal surfaces, which can cause interference and detuning of the antenna (Finkenzeller, 2010). This poses a

challenge for designing RFID tag antennas that maintain optimal performance when mounted on or near metallic objects.

In summary, RFID systems provide an efficient and automated method for data collection, significantly enhancing operational efficiency in various industries. The technology continues to evolve, with ongoing research focusing on improving the performance of RFID tags, especially for challenging environments like metal-mountable applications.

2.3 General Antenna Design Principles

The fundamental goal in designing an RFID antenna is to achieve optimal performance across several key parameters. These elements ensure that the tag can communicate effectively with the reader, transmitting and receiving signals without significant losses. One of the most common designs for RFID tags is the patch antenna, known for its compact size, planar structure, and ease of integration into various applications (Balanis, 2016). Patch antennas are particularly advantageous in UHF RFID systems because they are capable of providing long read ranges and are relatively straightforward to manufacture.

2.3.1 Directional and Omnidirectional Antennas

Antennas are generally classified into directional and omnidirectional types based on their beamwidth characteristics. Beamwidth refers to the angular separation between the two 3 dB points of an antenna's radiation pattern, representing the effective coverage area of the antenna. Figure 2.2 illustrates the difference in coverage regions between directional and omnidirectional transmissions.

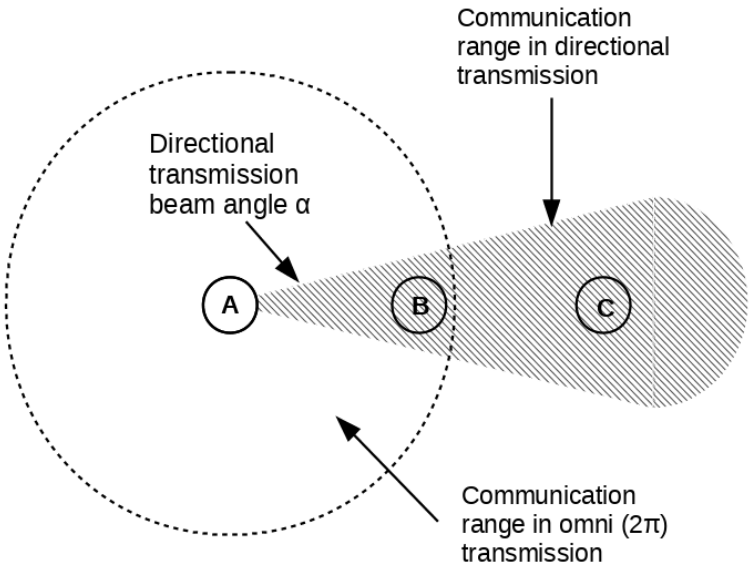

Figure 2.2: Coverage regions for directional and omnidirectional antennas.

Directional antennas concentrate most of their radiated energy in a specific direction, resulting in higher gain in that direction. This makes them highly effective in applications where the communication link is fixed or where long-distance coverage is required. For example, Yagi-Uda antennas and parabolic reflectors are commonly used in scenarios such as point-to-point communication or satellite systems (Balanis, 2016). However, the focused beam of directional antennas can limit their versatility in environments where the antenna's orientation or the tag-reader alignment changes frequently. In the context of RFID systems, directional antennas are often employed in portals or gates where items pass through a predefined path. Their high gain allows the RFID reader to detect tags from a significant distance, ensuring reliable operation even in noisy environments. Nonetheless, the need for precise alignment can introduce challenges in dynamic or unpredictable setups (Dobkin, 2012).

Omnidirectional antennas, on the other hand, radiate energy uniformly in all directions within a plane, usually the azimuth plane. This characteristic makes them well-suited for applications requiring 360° coverage, such as wireless access points or mobile communication devices (Finkenzeller, 2010). For UHF RFID systems, omnidirectional antennas are advantageous in environments where tags may approach from any direction, ensuring consistent detection without the need for orientation adjustments.

The trade-off with omnidirectional antennas is their lower gain compared to directional antennas, as the energy is distributed over a broader area. However, their flexibility and ease of deployment make them a popular choice for applications like inventory management in warehouses, where items can be scattered or moved unpredictably.

2.3.2 Antenna Gain and Read Distance

Antenna gain is a critical parameter in determining the efficiency and effectiveness of an RFID system. It represents the ability of the antenna to focus radiated power in a specific direction compared to an isotropic radiator. Gain is defined as the ratio of the radiation intensity in a given direction to the radiation intensity of an isotropic source under the same power input (Balanis, 2016). It is usually measured in decibels relative to an isotropic source (dBi). Antennas with higher gain are typically designed for directional radiation patterns, concentrating energy in a specific direction. For instance, directional antennas used in RFID portals can achieve higher read distances by focusing energy on a narrow beam. However, this comes at the cost of reduced coverage in other directions (Dobkin, 2012).

The read distance of an RFID tag depends on several factors, including antenna gain, transmitted power, tag sensitivity, and environmental conditions. Higher antenna gain improves the read distance by focusing more energy on the tag, enabling stronger backscatter signals to be received by the reader (Dobkin, 2012). However, environmental factors such as interference from metal surfaces or signal absorption by liquids can also affect the read range. The Friis transmission equation provides a mathematical basis for understanding the relationship between antenna gain and read distance. It can be expressed as:

$$P_r = P_t G_t G_r \left(\frac{\lambda}{4\pi r}\right)^2 \quad (2.1)$$

Where

P_r = power received by the tag, W

P_t = power transmitted by the reader, W

G_r = gain of the reader antenna, unitless

G_t = gain of the tag antenna, unitless

λ = wavelength of the signal, m

r = distance between the reader and the tag, m

2.3.3 Radiation Efficiency

Radiation efficiency represents how effectively an antenna converts input power into radiated electromagnetic energy. It serves as a key metric for evaluating overall antenna performance. However, for electrically small antennas, radiation efficiency is inherently limited due to increased reactive fields and ohmic losses, which constrain the amount of power that can be efficiently radiated.

On the other hand, poor conductivity in metallic components or high dielectric loss in substrates, power reflection caused by impedance mismatch, reflections, absorption, or detuning effects caused by proximity to metallic surfaces or high-permittivity materials can result in reduced efficiency.

2.3.4 S-Parameter, Impedance Matching and Resonant Frequency

The S-parameter, particularly S_{11}, is a measure of the reflection coefficient at the input port of the antenna. It represents the fraction of power reflected back into the source due to impedance mismatch. A lower S11 value (typically below -10 dB) indicates better impedance matching and efficient power transfer between the antenna and the feed line or RFID chip (Balanis, 2016).

Impedance matching is critical to minimize power reflection and maximize power transmission. According to the Maximum Power Transfer Theorem, maximum power transfer occurs when the impedance of the antenna ($\boldsymbol{Z}_A$) equals the complex conjugate of the chip impedance ($\boldsymbol{Z}_c^*$):

$$\boldsymbol{Z}_A = \boldsymbol{Z}_c^* \tag{2.2}$$

Where

$\boldsymbol{Z}_A$ = input impedance of the antenna, Ω

$\boldsymbol{Z}_c$ = impedance of the chip, Ω

In this condition, the reflected power is minimized, resulting in the lowest S_{11} value and efficient energy transfer to the antenna. As impedance matching achieved, the capacitive reactance and inductive reactance cancel

each other out, will result in resonant frequency. Figure 2.3 show the resonant frequency of the antenna.

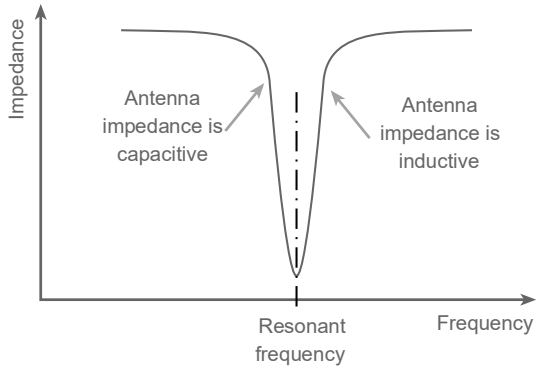

Figure 2.3: Resonant frequency of the antenna. (Electronic notes, 2024)

The resonant frequency of the antenna is determined by its geometry, material properties, and environmental factors. For RFID systems in this project, this frequency is designed to fall within the UHF band (902-928 MHz) to meet the standards.

2.3.5 Bandwidth

Bandwidth refers to the range of frequencies over which an antenna operates efficiently, maintaining acceptable performance in terms of impedance matching, gain, and radiation characteristics. It is typically defined as the frequency range where the reflection coefficient (S_{11}) remains below a specified threshold, commonly −10 dB. In UHF RFID systems, the antenna bandwidth must cover the designated operating range—for example, 902–928 MHz in FCC-regulated regions—to ensure consistent and reliable tag performance (Finkenzeller, 2010). Figure 2.4 illustrates an example of reflection coefficient (S_{11}) plotted versus frequency.

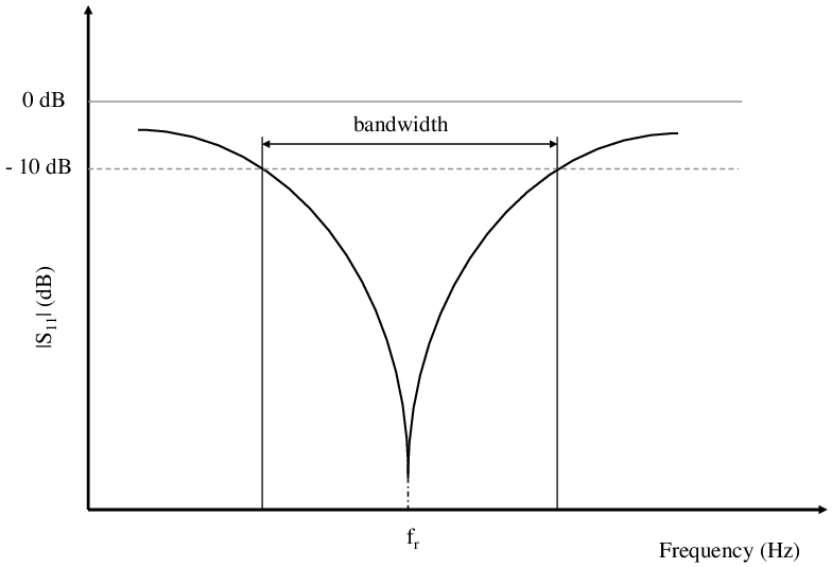

Figure 2.4: Reflection coefficient (S_{11}) graph versus the frequency.

The bandwidth of an antenna is influenced by its design and material properties. Antennas with high-quality substrates and optimized geometries tend to exhibit broader bandwidths. However, achieving wide bandwidth can be challenging in compact antennas, where size constraints often limit performance.

2.4 Patch Antennas

2.4.1 Patch Antenna Design

A patch antenna typically consists of a conducting patch placed on top of a dielectric substrate, with a ground plane underneath the substrate. The patch is usually made of metal and can take various shapes, such as rectangular, circular, or triangular, depending on the design requirements. The fundamental working principle of patch antennas is based on the radiation of electromagnetic waves from the edges of the conducting patch. The radiation is generated when the electric and magnetic fields in the patch resonate at specific frequencies, determined by the physical dimensions of the patch and the properties of the dielectric material (Balanis, 2016).

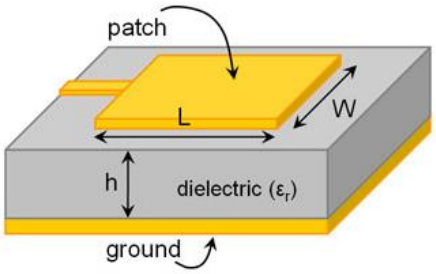

Figure 2.5: Microstrip Patch Atenna. (www.emtalk.com, n.d.)

The dimensions of the patch are generally a fraction of the operating wavelength, making patch antennas compact and suitable for portable devices such as RFID tags. A key factor in patch antenna design is the operating frequency, which dictates the size of the antenna. For UHF RFID applications, patch antennas are typically designed to operate in the 902 MHz to 928 MHz range, which corresponds to the UHF RFID passbands.

There are various methods for feeding patch antennas, each with its advantages and design considerations. The most common feeding techniques include: Microstrip Line Feeding, Coaxial Probe Feeding, Proximity Coupling. In Microstrip Line Feeding, a microstrip line is printed on the dielectric substrate and connected to the edge of the patch. This method is easy to design and fabricate but may suffer from impedance mismatch and radiation losses (Pozar, 2012). In Coaxial Probe Feeding, A coaxial cable is fed through the ground plane and dielectric substrate, with the inner conductor connected to the patch. This method provides better impedance matching and less spurious radiation but requires precision in drilling the substrate (Garg et al., 2001). While Proximity Coupling involves placing a microstrip line below the patch and coupling the energy through the dielectric substrate. This technique offers improved bandwidth and isolation between the feed and the radiating patch but is more complex to design (Balanis, 2016).

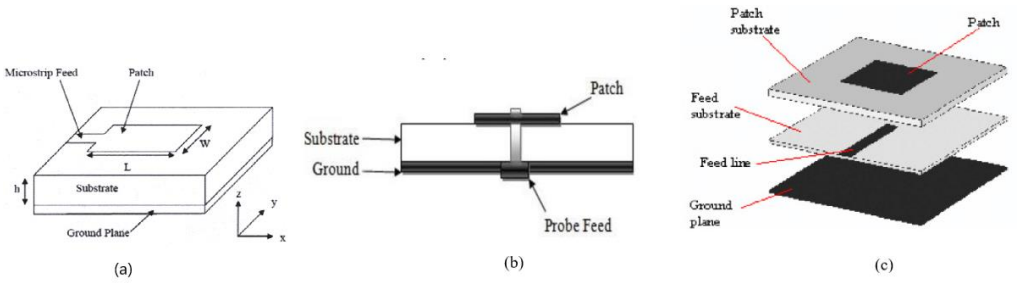

Figure 2.6: (a) Microstrip Line Feeding, (b) Coaxial Probe Feeding, (c) Proximity Coupling.

2.4.2 Patch Antenna Performance on Metallic Surfaces

Traditional patch antennas typically suffer from performance degradation due to the strong reflection and interaction with surface currents on the metal when placed on metallic surfaces. These antennas are not inherently designed to handle such conditions, which can result in issues like reduced gain and poor impedance matching.

In contrast, metal-tolerant designs incorporate features that help maintain performance even in the presence of metallic surfaces. Metal-tolerant patch antennas often include additional layers of dielectric material or high-impedance surfaces to prevent direct interaction with the metal. Additionally, these antennas may be designed with specialized feeding techniques to ensure proper impedance matching and minimal radiation loss (Foster and Burberry, 2004). These designs are particularly beneficial in UHF RFID systems, where tags are frequently mounted on metallic objects such as containers and machinery.

2.5 Metal-Mountable RFID Tag Antennas

RFID systems mounted on metallic surfaces face unique challenges, such as altered electromagnetic field distributions, leading to poor antenna performance. Significant research has been conducted to address these issues by designing specialized antennas that function well in such environments. Many early designs of metal-mountable RFID antennas, such as patch antennas with dielectric spacers, were developed to reduce interference caused by the metal surface and to maintain consistent antenna performance. These designs focus on maintaining high read ranges, low-profile structures, and

sufficient impedance matching even when the tag is attached to metallic surfaces (Karmakar, 2010).

One common approach is the use of dielectric spacers, where a layer of dielectric material is inserted between the antenna and the metallic surface to reduce electromagnetic interference and mitigate detuning effects. Another effective solution involves the use of artificial magnetic conductors (AMCs) or high-impedance surfaces, which minimize the interaction between the tag and the metal surface. These surfaces act as electromagnetic shields, reflecting signals without generating destructive interference, thus improving antenna performance. Various research studies have demonstrated the effectiveness of this approach in mitigating the negative effects of metal surfaces on antenna performance (Chen et al., 2009).

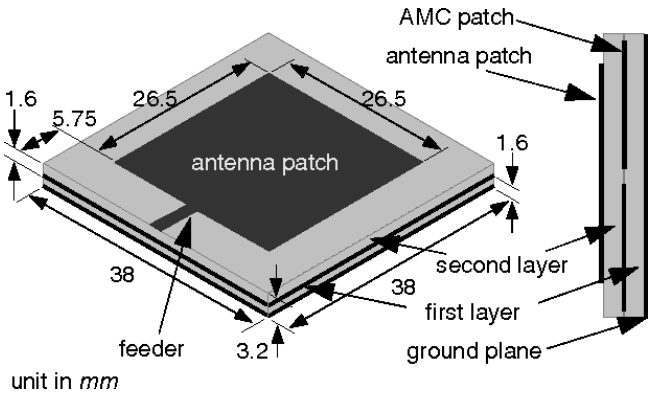

Figure 2.7: Patch Antenna with AMC Structure. (Ihsan & Munir, 2020)

However, these solutions are not without limitations. The added complexity of including dielectric layers or AMCs can increase the cost and size of the tag, which may not be ideal for applications where a compact design is required. Furthermore, many of these designs are highly specific to certain metal surfaces, and their performance may vary significantly when mounted on different types of metallic objects.

Recently, zeroth-order resonator (ZOR) antennas have emerged as a promising solution for metal-mountable applications. These antennas achieve resonance independent of their physical size, enabling compact designs that maintain high radiation efficiency even when mounted on metal surfaces. ZOR

antennas also provide omnidirectional radiation patterns above the surface, ensuring reliable operation in dynamic industrial environments.

2.6 Zeroth-Order Resonator (ZOR)

2.6.1 Resonators

Resonance is a phenomenon that occurs when a system oscillates with greatest amplitude at specific frequencies, known as resonant frequencies. This happens due to the constructive interference of oscillatory energy, where the natural frequency of the resonator aligns with the frequency of an external excitation. A resonator typically refers to a homogeneous object in which waves propagate at an approximately constant velocity, reflecting back and forth between boundaries. These oppositely traveling waves interfere with each other, and at the resonant frequencies, they reinforce one another to form standing wave patterns within the resonator. As illustrated in Figure 2.9, the condition for resonance in a resonator can be expressed as:

$$d = \frac{n\lambda}{2},\ n \in \mathbb{Z} \tag{2.3}$$

Therefore, the resonant frequencies (f) and phase constant (β) are:

$$f = \frac{c}{\lambda} = \frac{nc}{2d},\ n \in \mathbb{Z} \tag{2.4}$$

$$\beta = \frac{2\pi}{\lambda} = \frac{n\pi}{d},\ n \in \mathbb{Z} \tag{2.5}$$

Where

d = distance between the sides of resonator, m

λ = wavelength, m

f = resonant frequency, Hz

c = velocity of the wave, ms^{-1}

β = phase constant, $radm^{-1}$

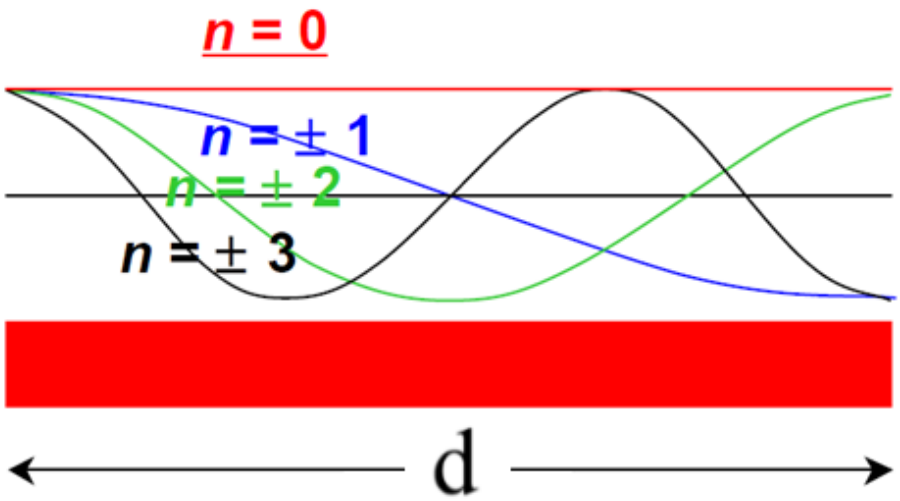

Figure 2.8: Resonant modes in resonator. (Sanada, Caloz and Itoh, 2003)

The lowest resonant frequency called fundamental frequency (n = 1), the higher allowable frequencies are entire number of multiples in a fundamental frequency, called harmonic. It is important to note that the fundamental frequency is defined as the frequency corresponding to n = 1, but not n = 0. While mathematically, the condition n = 0 is permissible in wave equation. It does not correspond to typical physical resonance behavior. When n = 0, the phase constant (β) becomes zero, resulting in a scenario where the wavelength (λ) becomes theoretically infinite. This means no physical standing wave pattern can form, as the wave effectively does not oscillate.

However, this special case has practical significance in engineered systems like Zeroth-Order Resonators (ZORs). In ZOR systems, resonance occurs even when n = 0, not due to the wavelength of the EM wave, but due to the unique properties of the resonator's geometry or materials, such as the Composite Right/Left-Handed (CRLH) transmission line. In these cases, resonance is independent of the physical dimensions of the resonator, which enables the design of compact and efficient antennas, making ZORs particularly advantageous for applications with strict size constraints.

2.6.2 Composite Right/Left-Handed Transmission Line (CRLH-TL)

Transmission lines are essential components in electromagnetic systems, serving as pathways for signal propagation. Traditional transmission lines can

be categorized as right-handed (RH) or left-handed (LH) based on the phase and group velocity relationship. A right-handed transmission line (RH-TL) exhibits conventional properties where the phase velocity and group velocity travel in the same direction. The series inductance (L_R) and shunt capacitance (C_R) of an RH-TL are associated with the natural inductive and capacitive behavior of the line (Pozar, 2012). Figure 2.10 (a) shows the equivalent circuit model (unit cell) of Homogeneous RH-TL. The phase constant (β) of Homogeneous RH-TL can be expressed as:

$$\beta = \omega\sqrt{L'_R C'_R} \tag{2.6}$$

Where

β = phase constant, $radm^{-1}$

ω = angular frequency, $rads^{-1}$

L'_R = series inductance per unit length, Lm^{-1}

C'_R = shunt capacitance per unit length, Cm^{-1}

In contrast, a left-handed transmission line (LH-TL) is an artificial medium where the phase velocity and group velocity are in opposite directions. This unique property is achieved by engineering the transmission line to exhibit effective negative inductance (L_L) and capacitance (C_L). LH-TL support backward-wave propagation and are often realized using periodic structures, such as series capacitors and shunt inductors, which enable them to exhibit properties not found in natural materials (Christophe Caloz and Itoh, 2002). Figure 2.10 (b) shows the equivalent circuit model (unit cell) of Homogeneous LH-TL. The phase constant (β) of Homogeneous LH-TL can be expressed as:

$$\beta = -\frac{1}{\omega\sqrt{L'_L C'_L}} \tag{2.7}$$

Where

β = phase constant, $radm^{-1}$

ω = angular frequency, $rads^{-1}$

L'_L = shunt inductance per unit length, Lm^{-1}

C'_L = series capacitance per unit length, Cm^{-1}

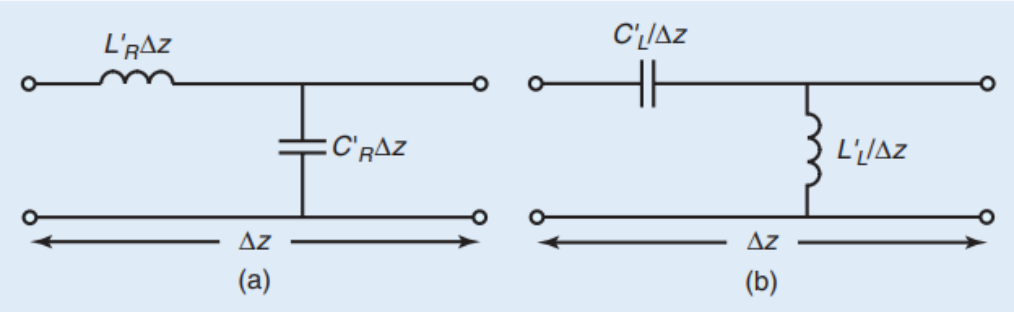

Figure 2.9: Equivalent circuit model (unit cell). (a) Homogeneous RH-TL, (b) Homogeneous LH-TL.

The composite right/left-handed transmission line (CRLH-TL) combines the characteristics of both RH and LH transmission lines. As shown in Figure 2.11, it consists of distributed elements that simultaneously exhibit right-handed and left-handed behavior, depending on the frequency of operation. At lower frequencies, the structure behaves as a left-handed medium due to the dominance of the series capacitors and shunt inductors. At higher frequencies, the inherent inductance and capacitance of the RH components take over, leading to right-handed propagation. The transition between LH and RH behaviors creates a balanced structure capable of supporting zeroth-order resonance (ZOR) and broadband operation (Lai, Caloz and Itoh, 2004).

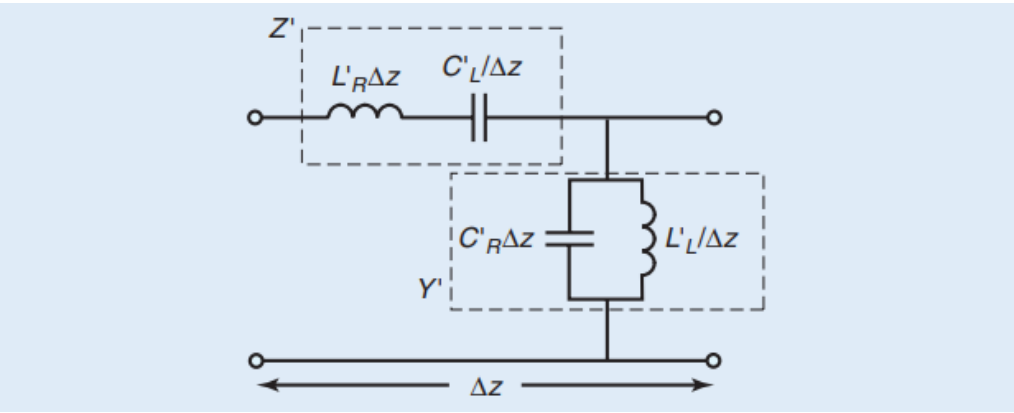

Figure 2.10: Equivalent circuit model (unit cell) of Homogeneous CRLH-TL.

It is evident that when the resonant frequency of the series components and shunt components are equal, a unique condition arises. At this frequency, the series components act as a short circuit, while the shunt

components behave as an open circuit. This condition allows the transmission line to achieve zeroth-order resonance, where the phase constant (β) becomes zero, and the theoretical wavelength (λ) approaches infinity. The critical condition for achieving same resonant frequency of the series components and shunt components can be expressed as:

$$L'_R C'_L = L'_L C'_R \tag{2.8}$$

The resonant frequency under this condition is:

$$f = \frac{1}{2\pi\sqrt[4]{L'_R C'_L L'_L C'_R}} = \frac{1}{2\pi\sqrt{L'_R C'_L}} = \frac{1}{2\pi\sqrt{L'_L C'_R}} \tag{2.9}$$

Where

L'_R = series inductance per unit length, Lm^{-1}

C'_R = shunt capacitance per unit length, Cm^{-1}

L'_L = shunt inductance per unit length, Lm^{-1}

C'_L = series capacitance per unit length, Cm^{-1}

f = resonant frequency, Hz

2.6.3 ZOR Antennas

Zeroth-Order Resonator (ZOR) antennas are a unique class of antennas that operate based on zeroth-order resonance. The working principle of ZOR antennas is rooted in Composite Right/Left-Handed (CRLH) transmission line theory. Unlike conventional resonant antennas, which rely on their physical dimensions to determine their operating frequency, ZOR antennas achieve resonance independently of their size. Besides, The zeroth-order mode provides uniform field distribution and stable radiation characteristics. These unique properties allows for the design of highly compact and efficient antennas suitable for applications where space constraints are critica.

The design of a ZOR antenna involves replacing the lumped inductance and capacitance of a CRLH-TL with distributed elements in a microstrip structure. Instead of using discrete inductors and capacitors, different parts of the microstrip antenna itself serve as equivalent inductive and capacitive elements. The gap or slot between the patch and the feed line functions as a series capacitance, mimicking the left-handed capacitance of a CRLH-TL. Similarly, a shorting via or shorting wall, which connects one edge of the patch to the ground plane, introduces shunt inductance, substituting for

the left-handed inductor. The ground plane and dielectric substrate also contribute to right-handed inductance and capacitance, which support conventional wave propagation. By carefully designing these elements, the antenna can achieve the unique zeroth-order resonance condition required for efficient operation (Sanada, Caloz and Itoh, 2003).

In most cases, only a single CRLH-TL unit cell is required to achieve resonance. This makes them much more compact compared to traditional multi-cell CRLH-TL structures. The use of a single unit cell ensures that the antenna resonates at zeroth-order mode, allowing it to radiate efficiently despite its small size. Additionally, ZOR antennas are well-suited for omnidirectional radiation applications because they provide a more uniform radiation pattern.

2.7 Advances in Compact RFID Tag Antennas

Recent advancements in RFID technology have driven the demand for compact and cost-effective RFID tag antennas that can still perform well when mounted on metal surfaces. Researchers have focused on miniaturizing RFID tag antennas by employing techniques such as antenna meandering, which increases the electrical length of the antenna while keeping its physical size small. Other methods include the use of inductive loading and metamaterials to further reduce the size of the antenna without compromising its performance (Chen and Chiau, 2010).

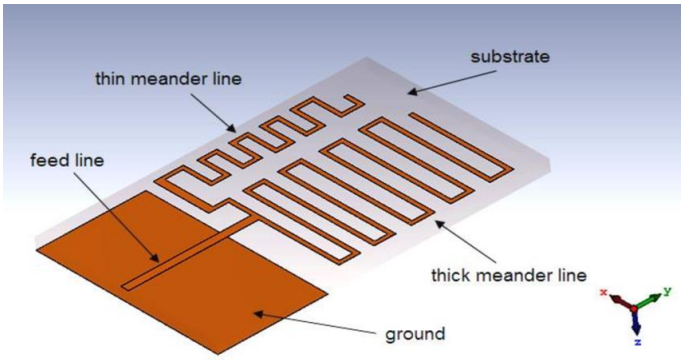

Figure 2.11: Antenna Meandering Technique in Patch Antenna. (Salih & Abdullah, 2022)

The integration of folded dipole structures and multi-layer designs has also shown promise in creating miniaturized antennas that can be used in metal-rich environments. These designs focus on maintaining a compact form factor while addressing issues such as impedance matching, radiation efficiency, and polarization.

The use of high-permittivity substrates is another effective method for reducing the physical size of antennas. By increasing the relative permittivity of the substrate, the wavelength of the resonant frequency within the material decreases, allowing the antenna's dimensions to be reduced without affecting its electrical characteristics. This technique is particularly advantageous for compact designs, as it helps maintain the desired operating frequency and impedance matching while minimizing the antenna's footprint.

2.8 Existing Solutions

2.8.1 Zeroth-Order Serpentine Antenna

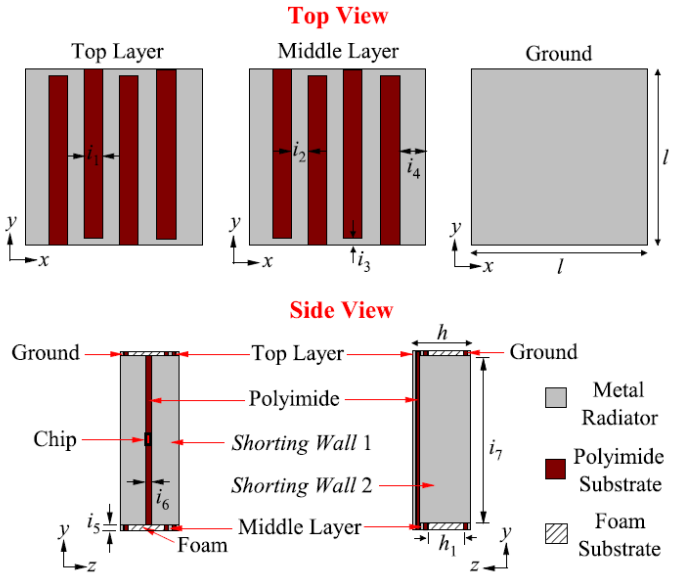

(a)

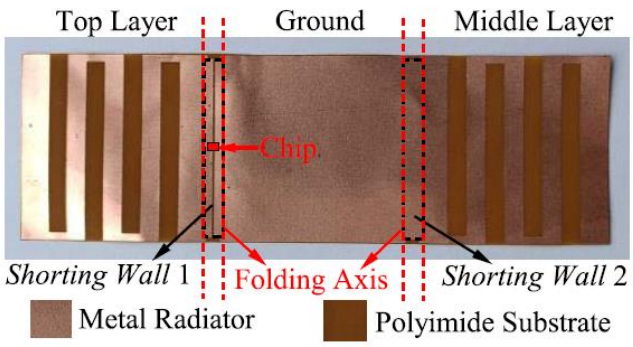

(b)

Figure 2.12: (a) Tag antenna configuration. (b) Single sided inlay.

The article introduces a zeroth-order resonant (ZOR) serpentine antenna designed for omnidirectional UHF RFID anti-metal tags, leveraging a double-layered serpentine structure folded around a low-permittivity foam substrate (Murugesh et al., 2021). This configuration comprises two closely stacked copper lines separated by a thin polyimide layer, generating strong capacitive reactance and parasitic elements critical for enabling zeroth-order resonance (ZOR).

The ZOR mode, facilitated by composite right/left-handed transmission line (CRLH-TL) characteristics, decouples the operating frequency from physical dimensions, allowing the antenna to resonate at 915 MHz despite its compact footprint (50 mm × 50 mm × 3.38 mm). Structural innovations include broad shorting walls replacing traditional stubs to stabilize impedance matching (achieving ~99% power transmission) and a folded geometry that simplifies fabrication while maintaining a low profile (0.010λ). The serpentine lines' inductive paths (L_R) and shorting walls' contributions to left-handed inductance (L_L) and capacitance (C_L) are tuned via line widths (i_2, i_3) to adjust resonance without altering the antenna's size.

Omnidirectional radiation arises from equivalent magnetic loop currents formed by apertures in the folded layers, ensuring uniform azimuthal coverage. The antenna demonstrates robust performance on metallic surfaces, achieving a consistent read range of 7.9–8.9 m with minimal sensitivity to backing materials or plate dimensions.

However, limitations include a relatively large footprint (50 mm ×50 mm), which may restrict use in space-constrained applications, and fabrication

complexity due to precise folding and stacking requirements, posing challenges for mass production. While the read range suffices for many scenarios, it may fall short in environments demanding longer detection distances.

2.8.2 Zeroth-Order Slot-Loaded Cap-Shaped Patch Antenna

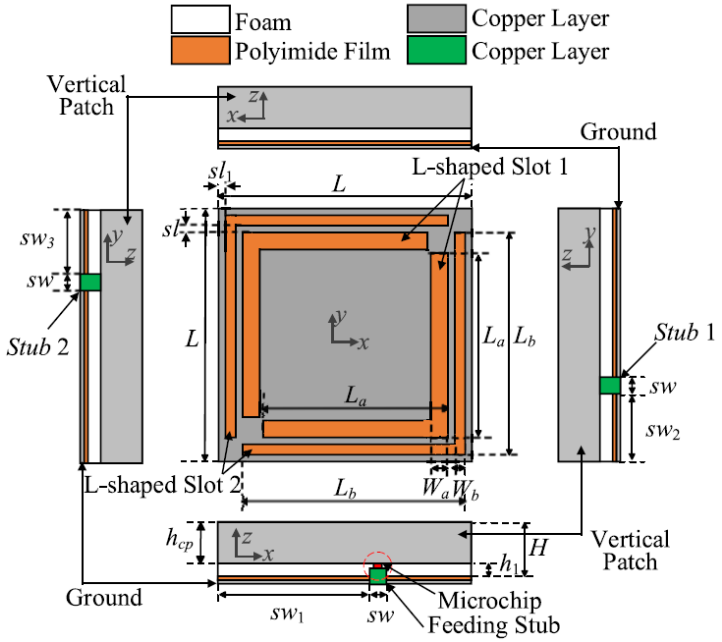

Figure 2.13: Schematic diagram of the proposed tag antenna.

The article presents a zeroth-order resonant (ZOR) UHF RFID tag designed for omnidirectional radiation when mounted on metallic surfaces (Ooi et al., 2023). The antenna features a cap-shaped patch etched with two pairs of L-shaped slots and is connected to the ground plane through two vertical inductive stubs. These structural elements introduce parasitic reactances (right-handed inductance, L_R , left-handed inductance, L_L , and right-handed capacitance, C_R) to enable zeroth-order resonance (ZOR), decoupling the operating frequency (915 MHz) from physical dimensions.

The ZOR mode is achieved through composite right/left-handed transmission line (CRLH-TL) characteristics, where the L-shaped slots elongate current paths to enhance inductive effects, while the stubs provide capacitive coupling. The antenna generates omnidirectional radiation via magnetic loop currents formed by equivalent magnetic currents $(\vec{M}_S =$

$-\vec{n} \times \vec{E}_a$) along sidewall apertures, mimicking a horizontal magnetic loop antenna. Key innovations include the single-element ZOR design for simplicity, vertically polarized fields on metal, and tunability via slot dimensions (L_a, L_b) to adjust resonance without altering footprint.

The antenna demonstrates a read range of 14.56 m in the azimuth plane with uniform spatial coverage and peaks at 19.18 m in elevation ($\theta = 50°$). It maintains stable performance across metallic plates of varying sizes and household metal containers, with minimal frequency drift (913–918 MHz).

However, limitations include a relatively high profile (4.8 mm) and footprint (44.8 mm × 44.8 mm), which may hinder use in space-constrained applications. The design relies on precise tuning of L-shaped slots for frequency adjustment, and fabrication involves complex folding of copper-clad polyimide layers, posing challenges for mass production.

2.9 Summary

In this chapter, a comprehensive review of the literature related to RFID systems, antenna design, and metal-mountable applications was conducted. The key principles behind RFID technology, particularly UHF RFID systems, were discussed, highlighting their advantages in various industrial applications. The challenges associated with designing antennas with omnidirectional radiation for metal surfaces, including impedance mismatch, detuning effects and lossing of omnidirectionality were identified as critical factors in achieving optimal performance.

Antenna design principles were examined, with an emphasis on patch antennas due to their compact size and ease of integration. Special attention was given to zeroth-order resonator (ZOR) Antenna, exploring their unique radiation characteristics and adaptability for compact designs. Recent advancements in RFID tag antenna technology, especially for metal-mountable applications, were also reviewed, revealing ongoing efforts to overcome metal interference through innovative solutions.

Despite significant progress in the field, gaps remain in designing compact, high-performance antennas for metal environments. These gaps provide the motivation for the current study, which aims to leverage ZOR

antenna principles to develop an efficient metal-mountable RFID tag antenna. The findings of this review underscore the need for continued exploration of miniaturized, robust antenna designs, with a focus on overcoming the specific challenges presented by metallic surfaces.

CHAPTER 3

METHODOLOGY AND WORK PLAN

3.1 Methodology

In the development of antenna systems, particularly for applications such as UHF RFID, a well-defined methodology is essential to achieving optimal performance. Initially, the process begins with requirement analysis, where the key performance parameters of the antenna are identified, including frequency range, bandwidth, gain, and radiation pattern. This phase involves understanding the specific needs and constraints of the application, such as environmental factors like metal surfaces or spatial limitations.

The next phase is conceptual design, where initial antenna designs are created based on the project's requirements. This includes selecting the appropriate antenna type and defining the basic dimensions and materials. The design is then refined through simulation and modeling, utilizing simulation software to predict the antenna’s behavior under various conditions and configurations. In this phase, the software CST Microwave Studio, which is an electromagnetic waves simulator, is used to design and simulate the proposed antenna design. This software can be used to design and develop the omnidirectional tag antenna. The characteristics such as the impedance and radiation characteristics of the proposed tag antenna can be observe and monitor by using the software.

Once the design is optimized, the next step is prototype fabrication, which involves constructing a physical model of the antenna based on the simulated design. This is typically done using techniques such as printed circuit board (PCB) manufacturing or 3D printing, depending on the material and structural requirements. After fabrication, the prototype is subjected to testing and evaluation to measure key performance parameters such as impedance matching, radiation pattern, and efficiency. This testing process verifies that the antenna functions as intended under real-world conditions and confirms that the design objectives have been successfully met.

The final phase, analysis and refinement, involves reviewing the test results and making any necessary adjustments to the design. This iterative process continues until the antenna meets all performance criteria. A structured approach to antenna design and testing is crucial for several reasons. It ensures that the antenna meets the specified performance criteria, reduces the risk of costly modifications or failures, improves efficiency by streamlining the design process, and provides reliable data for validating the antenna's performance. Furthermore, it supports iterative improvements, leading to a well-optimized final design.

3.2 Project Planning

This project is divided into four main stages. In the first stage, a comprehensive literature review is conducted, and the CST Studio Suite software is explored to gain familiarity with its simulation environment and capabilities. In the second stage, an UHF RFID tag antenna is designed and simulated using CST Studio Suite. In the third stage, the antenna parameters are further optimized using a conventional optimization algorithm to ensure that the tag exhibits a good omnidirectional radiation characteristic when mounted on metal surfaces. Finally, prototypes are fabricated and experimentally measured to validate the design.

This project aims to propose a novel UHF RFID tag antenna capable of achieving an omnidirectional radiation pattern, particularly in metal-mountable scenarios. To ensure timely completion of the project, a Gantt chart outlining the work plan has been developed. Table 3.1 and Table 3.2 displayed the gantt chart fot FYP1 and gantt chart for FYP2.

Table 3.1: Gantt chart for FYP 1.

No.	Project Activities	Planned Completion Date	W1	W2	W3	W4	W5	W6	W7	W8	W9	W10	W11	W12	W13	W14	W15	W16	W17
1.	Literature Study	2024-07-06																	
2.	Learning the CST Simulation Software	2024-07-20																	
3.	Learning How to Set Up a Simulation Model	2024-08-10																	
4.	Trying New Antenna Structure for Designing a RFID Tag Antenna	2024-09-07																	
5.	Preparing for Presentation	2024-09-21																	
6.	Doing Simulation for the New Antenna Structure	2024-10-12																	

Table 3.2: Gantt chart for FYP 2.

No.	Project Activities	Planned Completion Date	W1	W2	W3	W4	W5	W6	W7	W8	W9	W10	W11	W12	W13	W14	W15	W16	W17
1.	Optimizing and Finalizing Tag Antenna Design	2025-02-22																	
2.	Fabrication and Measurement	2025-04-19																	
3.	Writing Report and Conference Paper	2025-05-10																	
4.	Preparing for Final Presentation	2025-05-24																	

CHAPTER 4

RESULTS AND DISCUSSION

4.1 Introduction

Radio frequency identification (RFID) technology that operates in the ultra-high frequency (UHF) range has become a crucial component in industrial automation and inventory management due to its ability in wireless identification and object tracking. Commonly, the dipole has been used for designing tag antennas as they exhibit omnidirectional characteristic, which is useful for inventory management due to increased spatial coverage. However, mounting a dipole on a metallic object can experience degradation in radiation efficiency (Nguyen et al., 2021) as well as loss in omnidirectionality. To address these challenges, various on-metal omnidirectional UHF tag antennas that have a ground plane are proposed for mitigating the effects of the backing metal. Some of these designs include the use of the mushroom patch antenna (Tan et al., 2024) and the magnetic loop antenna (Lee et al., 2020). However, these designs are bulky, and they should be miniaturized further.

Recently, the application of the zeroth-order resonator (ZOR) antennas has emerged to be a promising solution due to their miniaturization capability (Li et al., 2020). By leveraging the unique properties of the ZOR, on-metal tag antennas that are designed using a single-element ZOR have been proposed. Two serpentine lines were overlapped for establishing a ZOR structure for generating omnidirectionality (Murugesh et al., 2021). A cap-shaped patch antenna, which is a mushroom structure in principle, was employed for designing an omnidirectional tag that was able to be read from a far read range (~ 15 m) (Ooi et al., 2023). However, the large footprint of the two antennas may limit their practical applications. Also, their omnidirectionality is slightly poorer as the gain variation in the azimuth plane is a bit higher (~ 1 dB) for both the tags.

In this part, a ZOR antenna has been proposed for designing an on-metal tag antenna with good omnidirectionality. The ZOR structure consists of two closely placed patches which are loaded with four L-shaped arms around its four corners. Two inductive lines are tactfully incorporated into the side

walls of the antenna for improving the electric fields distribution. By such means, improvement is seen in the omnidirectionality. This paper is organized as follows. Section 4.2 describes the antenna configuration. Section 4.3 presents the working principle. Section 4.4 presents the parametric analysis. Section 4.5 presents the simulated results of the optimized antenna. Section 4.6 presents the measurement results. Finally, a summary is drawn in Section 4.7.

4.2 Antenna Configuration

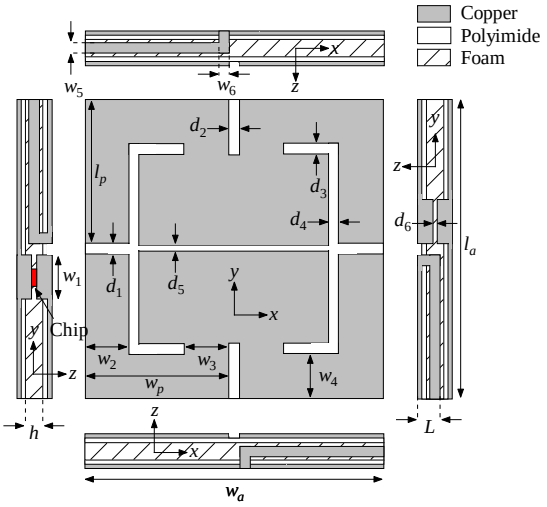

Figure 4.1: Tag antenna configuration. (l_a = w_a = 27, l_p = w_p = 13, d_1 = d_2 = d_3 = d_4 = 1, d_5 = d_6 = 0.5, w_1 = w_2 = w_3 = w_4 = 4, w_5 = w_6 = 1, L = 1.6, all parameters in mm).

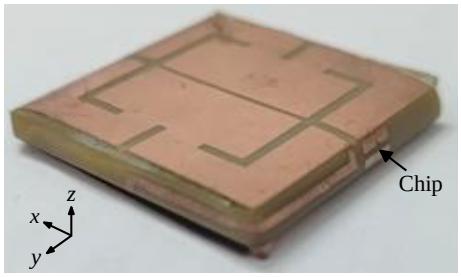

Figure 4.2: Snapshot of the prototype.

The structure of the proposed tag antenna is shown in Figure 4.1. The radiating element consists of a geometrically patterned copper layer with a thickness of 9 μm, which is etched on a single-sided copper-clad polyimide film with a thickness of 50 μm (DuPont, 2009). This inlay is subsequently folded and wrapped around a polyethylene (PP-2) foam (ECCOSTOCK, 2015) with ε_r =

1.03 and $tan\delta$ = 0.0001, which has a size of $l_a \times w_a$ (27 mm × 27 mm) and a thickness of h = 3.2 mm. As shown in Figure 4.1, the proposed tag consists of two rectangular patches that are closely placed with a narrow gap of d_5. The patches are then loaded with two pairs of L-shaped arms ($l_p \times w_p$) around its four corners. Finally, two highly inductive lines are loaded to the upper-left and lower-right side walls. To complete the design, a UCODE9 microchip (UCODE 9, n.d.) with an impedance of $10 - j191\ \Omega$ and a read sensitivity of –21.85 dBm is bonded, as shown from Figure 4.2.

4.3 Antenna Working Principle and Eigenmode Analysis

Table 4.1: Two Intermitent Tag antenna structures with their Radiation Patterns.

	Intermittent Antenna Configuration	3-D Gain Radiation (Logarithmic Scaling)
A	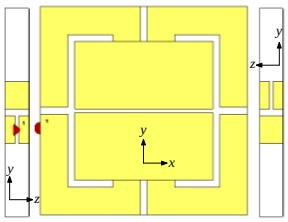	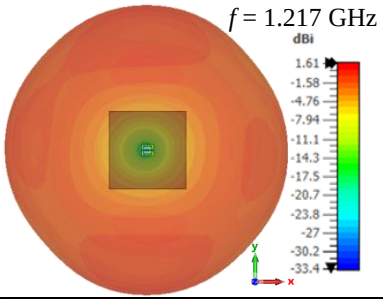
B	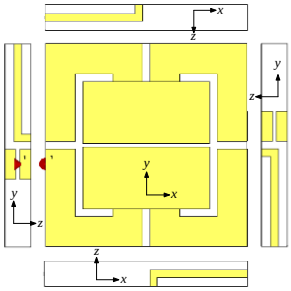	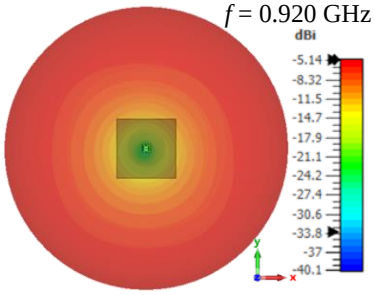

Table 4.2: Simulated surface currents and electric fields of antenna structures.

	Simulated Surface Currents	Simulated Electric Fields
A	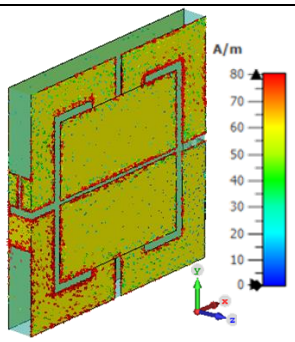	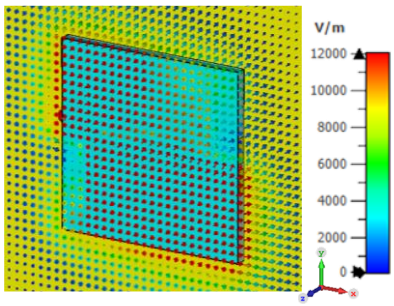
B	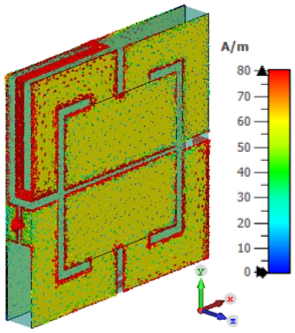	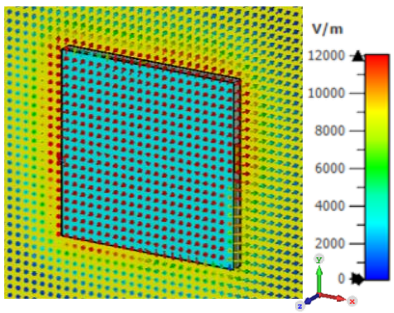

To elaborate the structural significance for achieving good omnidirectionality, analysis on the radiation patterns of two tag structures is performed at the zeroth-order mode, as shown in Table 4.1. The corresponding surface currents and electric fields are simulated in Table 4.2. An intermittent tag structure is first created by removing the two loading inductive lines on the two left and right walls, as shown in Case A. In this case, as observed in the tables, the omnidirectionality is observed to be compromised slightly. This is due to the uneven distribution of the electric fields around the four arms, as can be seen in Table 4.2. By appending two highly inductive lines on the left and right walls in Case B (Table 4.1), which is forming the final tag structure, the surface currents on the lower-left and upper-right arms are enhanced, causing the fields to distribute more evenly (Table 4.2). Due to this reason, the omnidirectionality has been significantly improved with a gain variation of only 0.205 dB, as seen in Table 4.1. Also observed is that high current density is observed in the two inductive lines, which has also successfully brought down the tag resonant frequency from 1.217 GHz to 0.920 GHz.

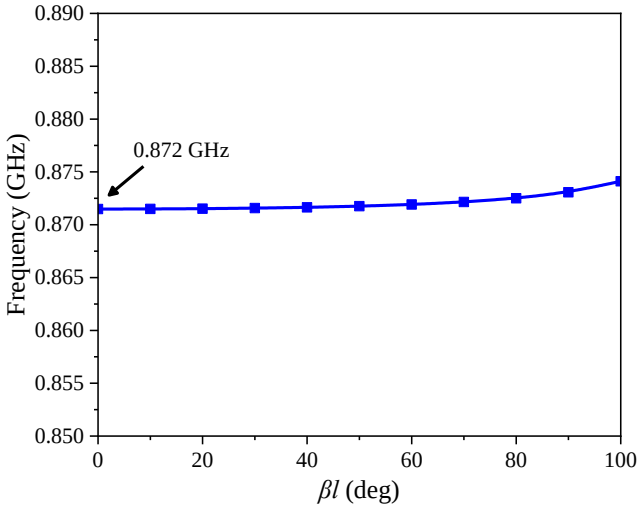

Figure 4.3:Simulated dispersion curve of the proposed tag antenna.

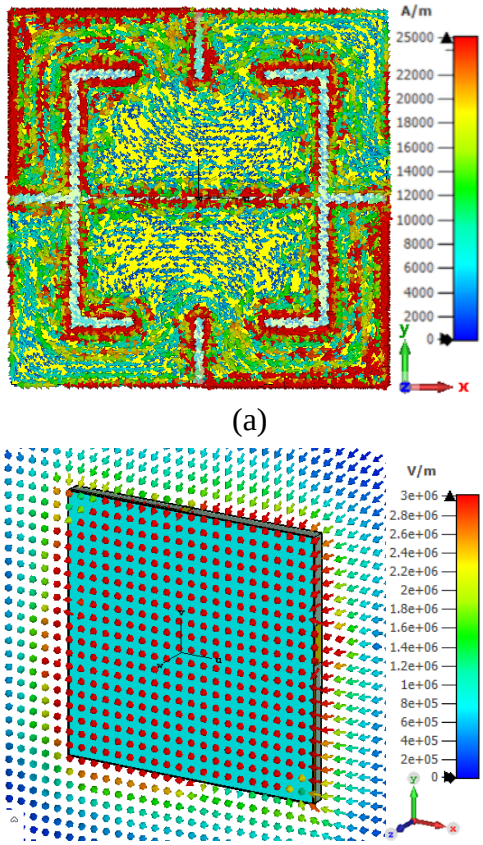

Figure 4.4: (a) Simulated currents and (b) electric fields in the eigenmode analysis.

To better understand the resonance characteristics of the proposed tag antenna, the chip is removed from the antenna structure, and it is placed inside a unit cell with a dimension of 120 mm × 120 mm × 32 mm according to the

specifications described (Ooi et al., 2023). Figure 4.3 presents the simulated dispersion curve as a function of the antenna's resonant frequency as well as its electrical length (βl). It can be observed that the ZOR frequency (βl = 0) is approximately 0.872 GHz, which is not far from the operating frequency (0.920 GHz) of the proposed tag antenna. Referring to Figure 4.3, the footprint of the antenna structure does not significantly affect its operating frequency, making it useful for miniature tag antenna design. This is also an important feature of the zeroth-order resonance. The surface currents and electric fields are simulated in the eigenmode analysis, as shown in Figure 4.4(a)-(b). The electric fields and surface currents are identical with those observed in Table 4.2 for antenna B, proving that the ZOR mode has been excited for the tag design.

4.4 Parametric Analysis

4.4.1 Patch Dimensions ($l_a \times w_a$)

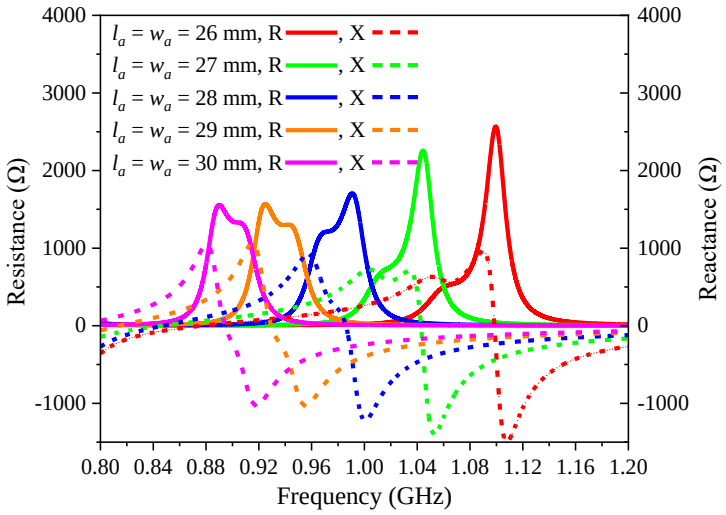

(a)

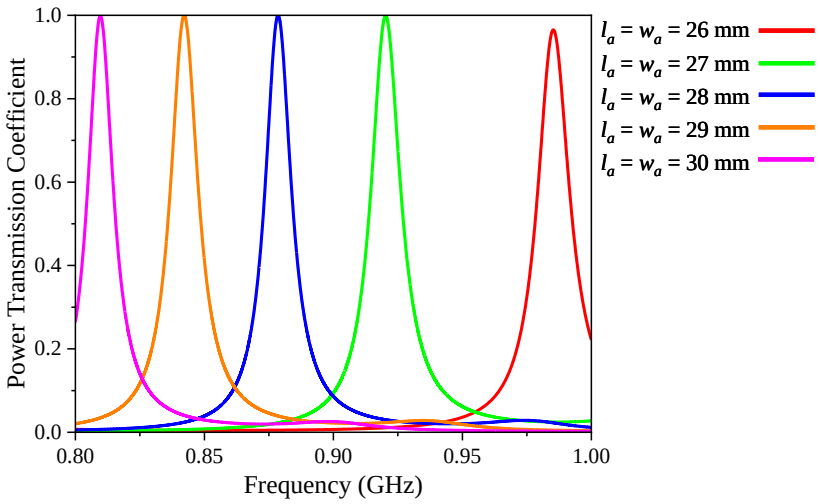

(b)

Figure 4.5: Impact of varying the patch dimension ($l_a \times w_a$) on (a) input impedance and (b) power transmission coefficient.

Parametric analysis was conducted to examine the effect of varying the patch dimensions ($l_a \times w_a$) on the antenna's input impedance and power transmission characteristics. As observed in Figure 4.5(a), increasing the patch dimensions ($l_a \times w_a$) causes the impedance curves shifts to left and lead to a decrease in resistance. In Figure 4.5(b), as the patch size ($l_a \times w_a$) increases from 26 × 26 mm^2 to 30 × 30 mm^2, the resonant frequency decreases with a tuning sensitivity of $\partial^2 f/\partial l_a \partial w_a = -43.9$ MHz/mm. Additionally, the power transmission coefficient shows a distinct peak at each resonant frequency, with higher values achieved when the antenna is better matched to the chip impedance.

Overall, the patch dimensions primarily affect the resonant frequency, which larger patch size result in lower resonant frequencies. However, in UHF RFID applications, the antenna size is often constrained by the need for compactness. When the antenna size is too small, its operating frequency tends to shift above the desired UHF range (902 MHz – 928 MHz). Therefore, additional parameters must be carefully tuned to bring the resonant frequency back within the target band but also to ensure proper impedance matching with the RFID chip.

4.4.2 Width of narraw gap (d_5)

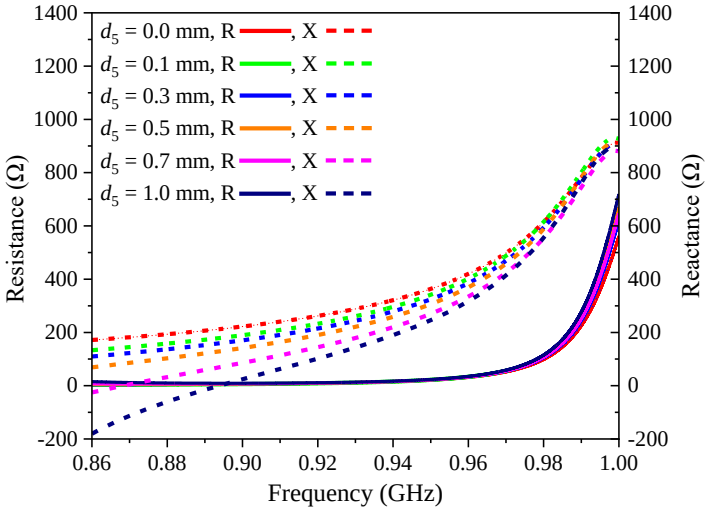

(a)

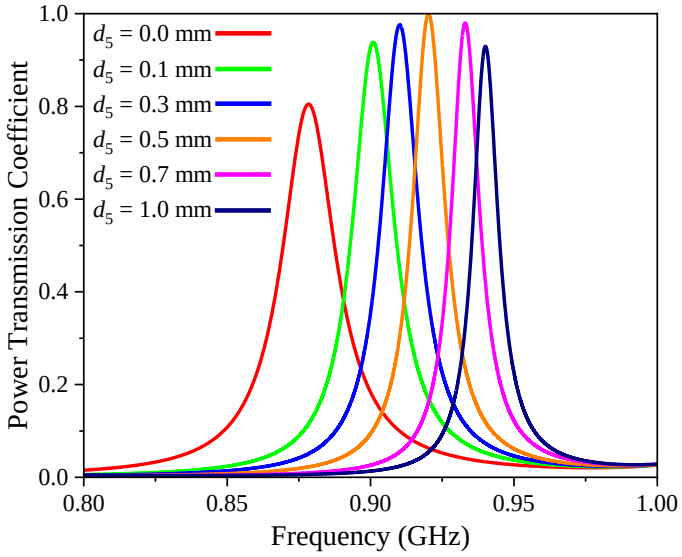

(b)

Figure 4.6: Impact of varying the width of narrow gap (d_5) on (a) input impedance and (b) power transmission coefficient.

As shown in Figure 4.6(a), increasing the width of the narrow gap (d_5) increases the reactance (X), while the resistance (R) remains relatively unchanged near the resonance frequency of 920 MHz. Changing d_5 allow for adjustment of the inductive reactance (X_L) at the rate of $\partial X_L/\partial d_5 = -160.0$ Ω/mm at 920 MHz. According to Figure 4.6(b), as the width of the narrow gap (d_5) increases from 0.0 mm to 1.0 mm, the resonant frequency increases with a tuning sensitivity of $\partial f/\partial d_5 = 61.6$ MHz/mm.

Notably, adjusting d_5 provides effective control over the impedance matching between the antenna and the RFID chip, as reflected by the variation in the power transmission coefficient shown in Figure 4.6(b). Therefore, d_5 served as a main paramter in tuning the impedance matching in this antenna design. Ensuring proper impedance matching is essential in maximizing power transmission from the reader to the RFID chip. While d_5 offers flexibility in impedance control, it also influences the resonant frequency. As a result, additional parameters must be tuned in parallel to maintain the resonance within the target UHF RFID band while optimizing overall performance.

4.4.3 Width of Highly Inductive Thin Lines (w_5)

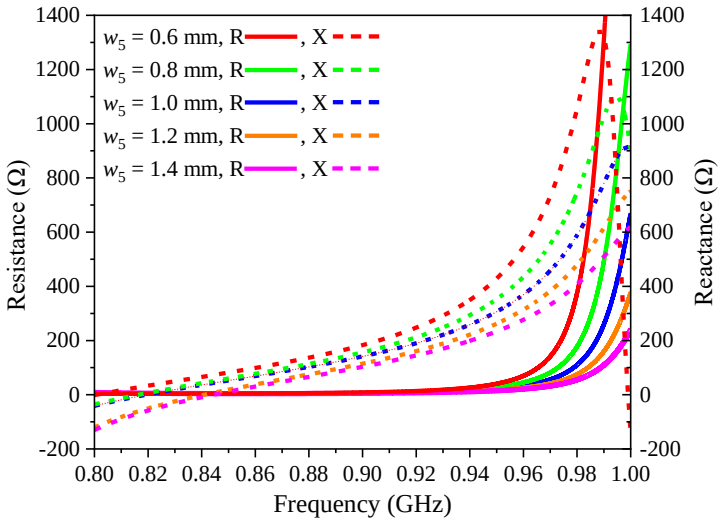

(a)

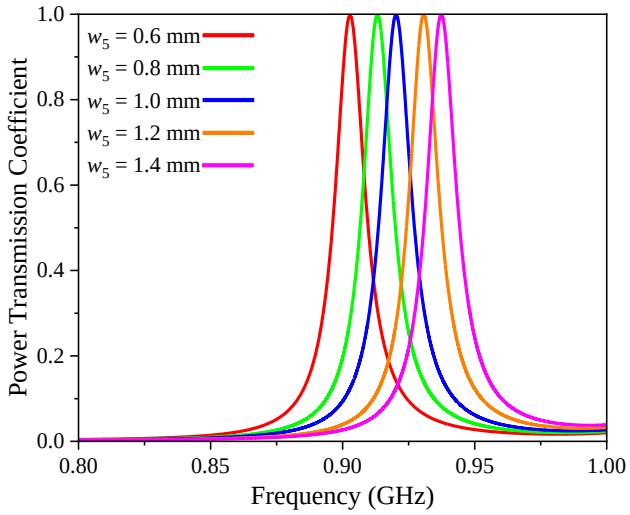

(b)

Figure 4.7: Impact of varying the width of highly inductive thin lines (w_5) on (a) input impedance and (b) power transmission coefficient.

According to Figure 4.7(a), increasing the width of the thin lines (w_5) increases the reactance (X), while the resistance (R) remains relatively unchanged near the resonance frequency of 920 MHz. Changing w_5 allow for adjustment of the inductive reactance (X_L) at the rate of $\partial X_L/\partial d_5 = -128.8\ \Omega$/mm at 920 MHz. In Figure 4.7(b), increasing the width of the thin lines (w_5) results in a tuning sensitivity of the resonant frequency, with $\partial f/\partial w_5 = 43.25$ MHz/mm. Despite this frequency shift, the power transmission coefficient remains nearly constant across different values of w_5, indicating stable transmission performance regardless of the thin line width.

Overall, the width of the highly inductive thin lines primarily affects the resonant frequency through its impact on the antenna's inductive characteristics. However, it is worth noting that the power transmission coefficient remains nearly constant across different values of w_5, indicating that this parameter has minimal influence on impedance matching. This stability in power transmission makes w_5 a useful tuning parameter for adjusting the resonant frequency without significantly affecting the antenna's matching performance. Therefore, w_5 serves as a secondary tuning element that can be leveraged to fine-tune frequency response after primary impedance matching has been achieved through other parameters such as d_5.

4.5 Simulated Results of the Optimized Antenna

4.5.1 S-Parameter and Resonant Frequency

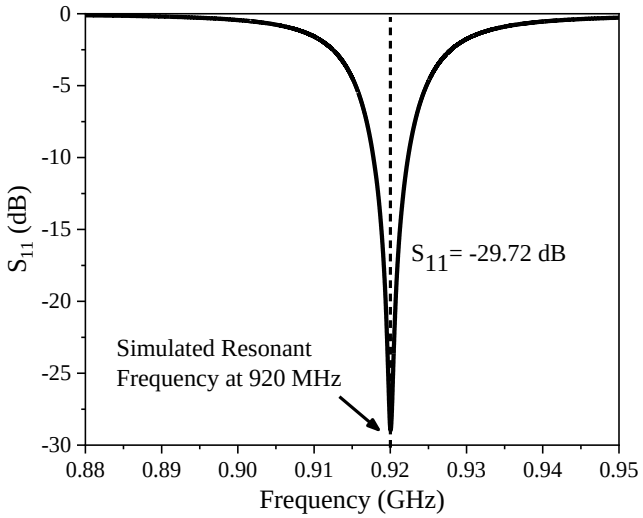

Figure 4.8: S-parameter versus frequency graph of the optimized antenna.

The S-parameter (S_{11}) versus frequency graph of the optimized tag antenna is presented in Figure 4.8. The reflection coefficient (S_{11}) has a minimum point at 920 MHz, indicating the resonance of the antenna occurred at this frequency. At resonance, the imaginary components of the antenna and the RFID chip cancel each other out, resulting in a purely resistive impedance. Furthermore, the reflection coefficient at this point is −29.72 dB, demonstrating good impedance between the RFID chip and the proposed tag antenna is achieved. As a result, a significant portion of the input power is successfully delivered to the antenna rather than reflected back.

4.5.2 Input Impedance

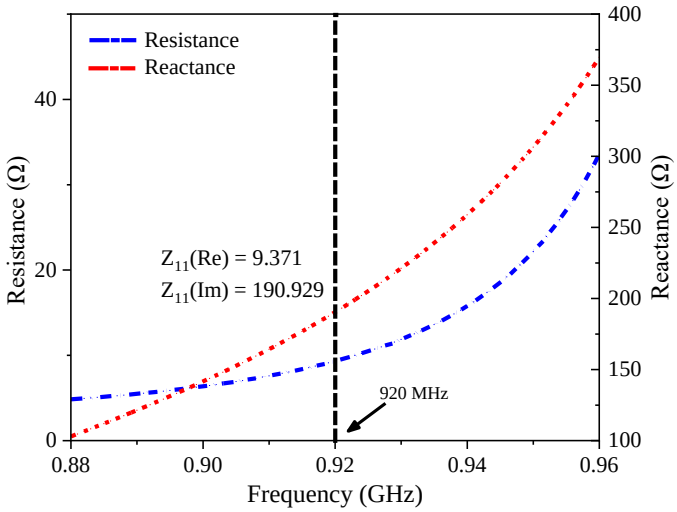

Figure 4.9: Input impedance of the optimized antenna.

The input impedance (Z_{11}) is simulated using CST Studio Suite software. According to Figure 4.9, the input impedance of the optimized antenna at the resonant frequency of 920 MHz is 9.371 + j190.929 Ω, which closely match the conjugate impedance of the UCODE 9 chip (10 − j191 Ω). This result demonstrates excellent impedance matching, ensuring maximum power transmission.

4.5.3 Power Transmission Coefficient

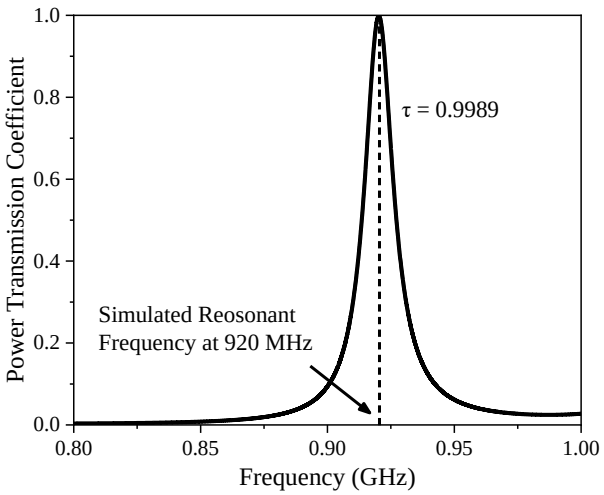

Figure 4.10: Power transmission coefficient of the proposed antenna.

The good impedance matching is further validated by analyzing the power transmission coefficient (τ) of the optimized tag antenna. According to Figure 4.10, the power transmission coefficient achieves 0.9989 at the resonant frequency of 920 MHz, meaning that 99.89% of the power from the RFID chip is efficiently transferred to the antenna. This high transmission efficiency confirms that the impedances of the antenna and chip are well-matched, minimizing reflection-related power loss and ensuring optimal performance of the tag in UHF RFID applications.

4.5.4 Radiation Pattern and Realized Gain

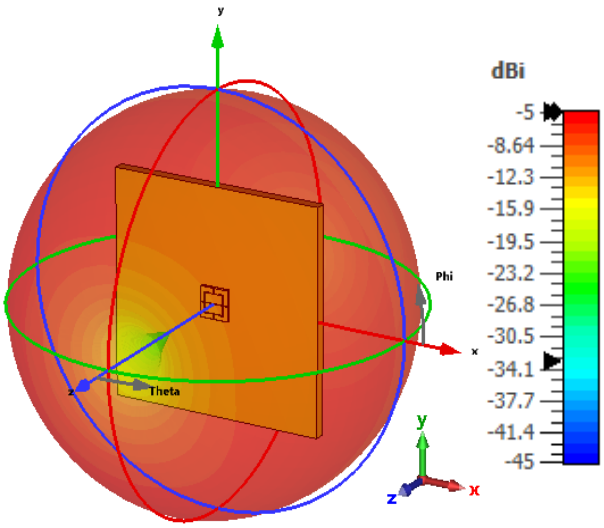

Figure 4.11: Simulated 3-D gain radiation characteristic of the optimized antenna.

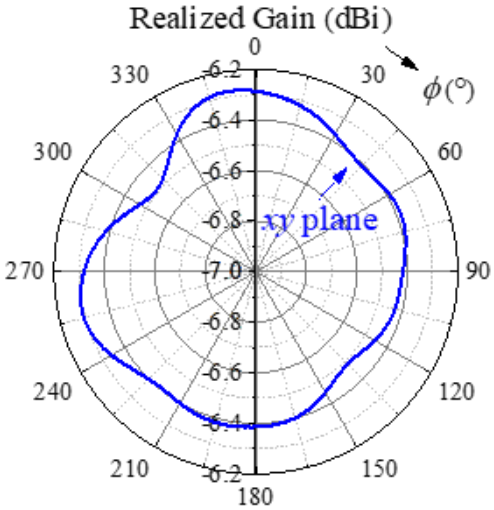

Figure 4.12: Simulated realized gain in the azimuth plane.

As shown in Figure 4.11, the proposed tag antenna exhibits a good omnidirectional characteristic. When mounted on an aluminium plate, the antenna achieves a realized gain of approximately −6.4 dBi, with a gain variation of only 0.2 dBi across different azimuth directions, indicating a fairly uniform radiation distribution, as illustrated in Figure 4.12. Additionally, the radiation efficiency is found to be 0.2324 at the resonant frequency of 920 MHz, which is considered a good efficiency for an electrically small antenna with dimensions of 27 mm × 27 mm × 3.2 mm. As a result, the proposed tag antenna is capable of achieving a theoretical read distance of approximately 9.8 m in all azimuth directions.

4.6 Measurement Results

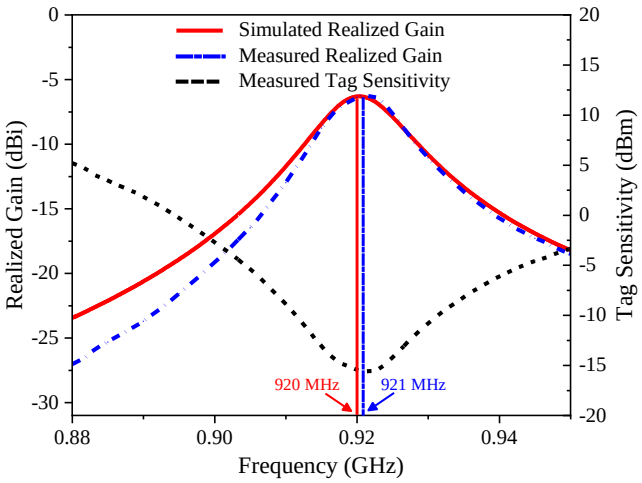

Figure 4.13: Measured and simulated realized gains along with the measured tag sensitivity.

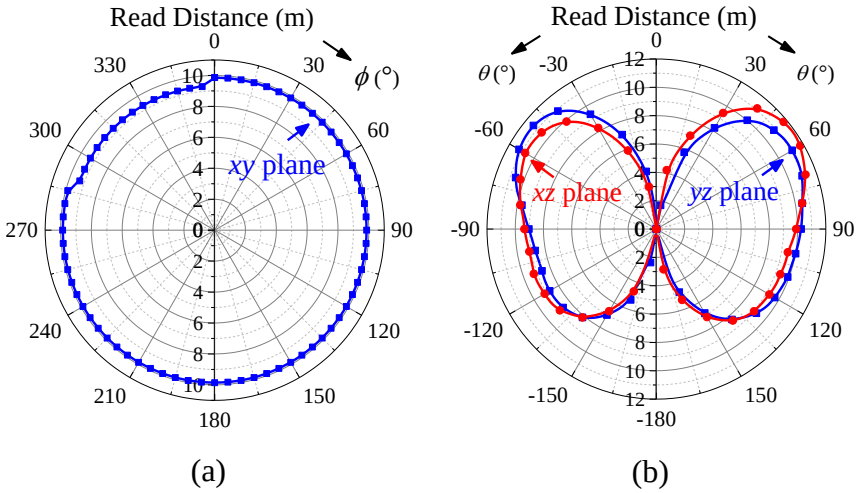

(a) (b)

Figure 4.14: Measured read patterns in the (a) *xy* plane, (b) *xz* plane and *yz* plane.

The prototype of the optimized tag antenna was manufactured. Its performance was characterised with the commercial RFID measurement system – Voyantic Tagformance (Voyantic Ltd., 2012). Throughout the experiment, the tag antenna was attached to an aluminium plate (20 cm × 20 cm × 1 cm). With reference to Figure 4.13, the simulated and measured resonant frequencies are 920 MHz and 921 MHz, respectively, with a difference of 1 MHz. The maximum achievable simulated and measured realized gains are –6.287 dBi and –6.225 dBi, respectively, with a difference of 0.062 dB. Next, the measured read patterns of the proposed tag antenna are shown Figure 4.14 (a)-(b) in the *xy*, *xz* and *yz* planes. It can achieve a maximum read range of ~9.8 m in the azimuth plane.

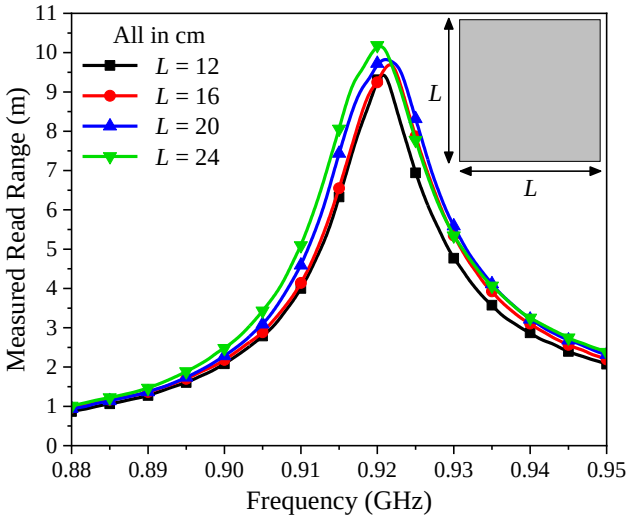

(a)

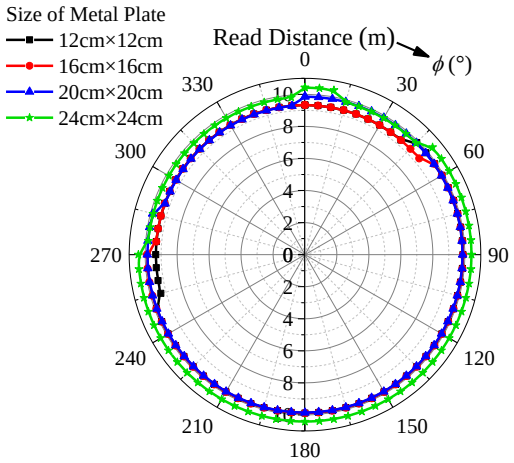

(b)

Figure 4.15: Measured (a) read ranges and (b) spatial read patterns of the proposed tag antenna in the *xy* plane when placed on different metal plates.

The prototype antenna was also tested on several square metallic plates, with the corresponding results shown in Figure 4.15 (a)-(b). Referring to Figure 4.15 (a), the tag has achieved a maximum read range of ~10.5 m and ~9.5 m, for the largest and smallest plate sizes, respectively. This is because changing the metal plate's size can slightly affect the read performance of the tag antenna, whereby a larger metal plate has resulted a longer read range. Similar trend was also seen in previous research (Murugesh et al., 2021), (Ooi et al., 2023). As shown in Figure 4.15(b), omnidirectional read pattern could be obtained when the proposed tag was measured on different plate sizes, with the read range recorded between ~9.5 m and ~10.5 m. Nevertheless, it is clear

that the tag resonant frequency remains stable at 921 MHz regardless of the metal plate’s size, indicating its usefulness for tagging metallic objects.

CHAPTER 5

CONCLUSIONS AND RECOMMENDATIONS

5.1 Conclusions

A compact ZOR tag antenna with a size of 27 mm × 27 mm × 3.2 mm has been proposed for designing an omnidirectional tag for on-metal tagging purposes. The excitation of the zeroth-order resonance has been verified through eigenmode analysis. The antenna consists of two rectangular patches, which are loaded with two pairs of L-shaped arms around the four corners. It has been shown that introducing the two highly inductive lines to the side walls has successfully improved the omnidirectionality by bringing down the gain variation to ~ 0.2 dB in the antenna's azimuth plane. When mounted on a metal, the antenna maintained a stable omnidirectional radiation charateristic with a realized gain of –6.225 dBi and an estimated read range of up to 9.8 meters across the entire azimuth plane. The proposed antenna has a operating frequency of 920 MHz and exhibits a high power transmission coefficient of 99.89% due to the good impedance matching. Overall, all design objectives of this study were successfully fulfilled.

5.2 Recommendations for future work

Although the proposed ZOR tag antenna has successfully achieved its design objectives, several improvements can be explored in future work. One key direction is bandwidth enhancement, as the current design operates optimally at 920 MHz with a relatively narrow bandwidth (~4.5 MHz). Expanding the bandwidth to cover the full UHF RFID range (902–928 MHz) would improve the antenna's versatility and ensure compatibility with global RFID systems. Another potential improvement is the development of multi-band operation, which would allow the antenna to support multiple RFID standards or even integrate other wireless functionalities, such as sensing or environmental monitoring. This could broaden the antenna's applications across different industries. Additionally, the antenna can be redesigned using flexible or stretchable materials to achieve flexible and conformal designs, enabling it to

be mounted on curved or irregular metal surfaces. This enhancement would make the antenna more suitable for real-world industrial scenarios, such as tagging cylindrical objects, machinery, or even biomedical equipment, where surface flatness cannot be guaranteed.

REFERENCES

Balanis, C.A., 2016. *Antenna Theory: Analysis and Design*. 4th ed. John Wiley & Sons.

Bong, F.-L., Lim, E.-H. and Lo, F.-L., 2017. Flexible Folded-Patch Antenna With Serrated Edges for Metal-Mountable UHF RFID Tag. *IEEE Transactions on Antennas and Propagation*, vol. 65, no. 2, pp. 647–653.

Chen, Q., Chiba, M., and Sawaya, K., 2009. Effects of metal plates and boxes on performances of RFID antennas. *IEEE Transactions on Antennas and Propagation*, 57(10), pp. 3303-3306.

Christophe Caloz and Itoh, T., 2002. Application of the transmission line theory of left-handed (LH) materials to the realization of a microstrip 'LH line'. *IEEE Antennas and Propagation Society International Symposium*. [ONLINE] Available at: https://ieeexplore.ieee.org/document/1016111. [Accessed 22 January 2025].

Cisco. 2020. *Omni Antenna vs. Directional Antenna - Cisco*. [ONLINE] Available at: https://www.cisco.com/c/en/us/support/docs/wireless-mobility/wireless-lan-wlan/82068-omni-vs-direct.html#topic3. [Accessed 14 January 2025].

Dobkin, D.M., 2012. *The RF in RFID: Passive UHF RFID in Practice*. 2nd ed. Elsevier.

DuPont., 2009. *DuPont™ Pyralux® AP All-Polyimide Flexible Laminate*. [ONLINE]. Available at: https://www.multi-circuit-boards.eu/fileadmin/pdf/leiterplatten_material/e_dupont_pyralux-ap-polyimid_www.multi-circuit-boards.eu.pdf [Accessed 10 Mar. 2025].

ECCOSTOCK PP, 2015. [ONLINE]. Available: https://www.laird.com/sites/default/files/2021-01/RFP-DS-PP%2006242020.pdf [Accessed 10 Mar. 2025].

Electronics notes. 2021. Antenna Resonance: Radio Aerial Bandwidth » Electronics Notes. [ONLINE]. Available at: https://www.electronics-notes.com/articles/antennas-propagation/antenna-theory/resonance-bandwidth.php. [Accessed 5 September 2024].

Finkenzeller, K., 2010. *RFID Handbook: Fundamentals and Applications in Contactless Smart Cards, Radio Frequency Identification and Near-Field Communication*. 3rd ed. John Wiley & Sons.

Foster, P. and Burberry, R., 2004. *Antenna Problems in RFID Systems*. Artech House, pp. 31–35.

Garg, R., Bhartia, P., Bahl, I. and Ittipiboon, A., 2001. *Microstrip Antenna Design Handbook.* Artech House, pp. 31–47

Ihsan, R.R. & Munir, A., 2020. Utilization of Artificial Magnetic Conductor for Bandwidth Enhancement of Square Patch Antenna. Proceedings of 2020 IEEE 10th International Conference on System Engineering and Technology (ICSET), Bandung, Indonesia, pp. 1-4. [ONLINE]. Available at: https://ieeexplore.ieee.org/stamp/stamp.jsp?tp=&arnumber=6366049 [Accessed 5 September 2024].

Karmakar, N.C., 2010. *Handbook of Smart Antennas for RFID Systems*. John Wiley & Sons, pp. 141–172.

Kwon, H. and Kim, B., 2004. Meandered microstrip RFID tag antenna for metallic objects. *Electronics Letters*, 40(19), pp.1097-1099.

Lai, A., Caloz, C. and Itoh, T., 2004. Composite right/left-handed transmission line metamaterials. *IEEE Microwave Magazine*, 5(3), pp.34–50. [ONLINE]. Available at: https://ieeexplore.ieee.org/stamp/stamp.jsp?tp=&arnumber=1337766. [Accessed 22 January 2025].

Lee, S.-R., Ng, W.-H., Lim, E.-H., Bong, F.-L. and Chung, B.-K., 2020. Compact Magnetic Loop Antenna for Omnidirectional On-Metal UHF Tag Design. *IEEE Transactions on Antennas and Propagation*, 68(2), pp.765–772.

Li, Z., Zhu, Y., Yang, H., Peng, G. and Liu, X., 2020. A Dual-Band Omnidirectional Circular Polarized Antenna Using Composite Right/Left-Handed Transmission Line With Rectangular Slits for Unmanned Aerial Vehicle Applications. *IEEE Access*, 8, pp.100586–100595.

Microstrip Patch Antenna Calculator, n.d. *em: talk* - [ONLINE]. Available at: https://www.emtalk.com/mpacalc.php. [Accessed 5 September 2024].

Muthukannan Murugesh, Lim, E.-H., Chee, P.-S. and Bong, F.-L., 2024. Zeroth-Order Serpentine Antenna With Omnidirectional Radiation Pattern for Anti-Metal Tag Antenna Design. *IEEE Journal of Radio Frequency Identification*, 8, pp.431–440.

Nguyen, M.-T., Lin, Y.-F., Chen, C.-H., Chang, C.-H. and Chen, H.-M., 2021. Shorted Patch Antenna With Multi Slots for a UHF RFID Tag Attached to a Metallic Object. IEEE Access, 9, pp.111277–111292.

Nikitin, P.V. & Rao, K.V.S., 2009. Antennas and propagation in UHF RFID systems. *Proceedings of the IEEE*, 98(9), pp. 1570-1582.

Ooi, S.-Y., Chee, P.-S., Lim, E.-H., Low, J.-H. and Bong, F.-L., 2023. A Zeroth-Order Slot-Loaded Cap-Shaped Patch Antenna With Omnidirectional Radiation Characteristic for UHF RFID Tag Design. *IEEE Transactions on Antennas and Propagation*, 71(1), pp.131–139.

Pozar, D. M., 2012. *Microwave engineering* (4th ed.). Wiley, pp. 300–306, 374–378.

Salih, A.A.K. & Abdullah, A.S., 2022. Design and Analysis of a Compact Dual-Band Printed Rectenna Circuit at WiFi and GSM Frequencies for Microwave Power Transmission. *Proceedings of the International Conference on Emerging Trends in Electrical, Electronics, and Communication Engineering*, University of Basrah, Iraq, pp. 1-6. [ONLINE]. Available at: https://www.researchgate.net/publication/369635836_Design_and_analysis_of_a_compact_dual_band_printed_rectenna_circuit_at_WiFi_and_GSM_frequencies_for_microwave_power_transmission [Accessed 5 September 2024].

Sanada, A., Caloz, C. and Itoh, T., 2003. *NOVEL ZEROTH-ORDER RESONANCE IN COMPOSITE RIGHT/LEFT- HANDED TRANSMISSION LINE RESONATORS*. [ONLINE] Available at: http://www.mwlab.ee.ucla.edu/publications/2003c/FB2_04.pdf [Accessed 20 Jan. 2025].

Shaban, H.F., Elmorsy, M., & Allam, A., 2011. UHF RFID antennas: Challenges for compact and metal-mountable designs. *Microwave and Optical Technology Letters*, 53(7), pp.1547-1550.

Tan, J.-I., Lee, Y.-H., Lim, E.-H., Bong, F.-L. and Chung, B.-K., 2024. A Low-Profile Top-Loaded Monopole Antenna for On-Metal RFID Tag Design. *IEEE Journal of Radio Frequency Identification*, 8, pp.448–457.

TT Electronics, 2022. *RFID: The Technology Making Industries Smarter | TT Electronics*. [ONLINE]. Available at: https://www.ttelectronics.com/blog/rfid-technology/. [Accessed 5 September 2024].

UCODE 9 Chip Data Sheet, Rev. 3.0, document SL3S1206, NXP, Eindhoven, Nederland, Dec. 2020.

Voyantic Ltd., 2012. *Tagformance Measurement System Manual 5*. Espoo: Voyantic Ltd.

Want, R., 2006. An introduction to RFID technology. *IEEE Pervasive Computing*, 5(1), pp.25-33. [ONLINE]. Available at: https://ieeexplore.ieee.org/stamp/stamp.jsp?tp=&arnumber=1593568 [Accessed 5 September 2024].